Materials Science

http://www.aimspress.com/journal/Materials/

AIMS Materials Science, 4(1): 89-101.
DOI: 10.3934/matersci.2017.1.89
Received: 30 October 2016
Accepted: 25 December 2016
Published: 05 January 2017

Research article

Effect of graphene substrate on the spectroscopic properties of photovoltaic molecules: role of the in-plane and out-of-plane π-bonds

Małgorzata Wawrzyniak-Adamczewska [1], Małgorzata Wierzbowska [2,*], and Juan José Meléndez [3]

[1] Faculty of Physics, A. Mickiewicz University, ul. Umultowska 85, 61-614 Poznań, Poland

[2] Institut of Physics, Polish Academy of Sciences (PAS), Aleja Lotnikow 32/46, 02-668 Warszawa, Poland

[3] Department of Physics and Institute for Advanced Scientific Computing of Extremadura (ICCAEX), University of Extremadura, Avenida de Elvas, s/n, 06006, Badajoz, Spain

[*] **Correspondence:** Email: wierzbowska@ifpan.edu.pl.

Abstract: The electronic structure of pentacene decorated with dipole groups (d-pentacene) and adsorbed onto a graphene substrate has been studied within the density functional theory. Three reference configurations have been considered, namely the ideal molecule without distortions, the actual molecule including intramolecular distortions and the molecule adsorbed onto graphene. Calculations show a noticeable charge redistribution within the d-pentacene + graphene system due to molecular distortion, as well as the formation of weak π-bonds between the molecule and the substrate. Additionally, the effect of the chemical modification of the terminal saturation with –H by –OH and =O is checked to explore the possibility of "levels engineering". The imaginary part of the dielectric function of d-pentacene in the ideal and distorted conformations and the molecule adsorbed at graphene were calculated within the random phase approximation. Results show that, even though molecular distortions change apreciably the absorption spectrum of isolated d-pentacene, the adsorbed molecule exhibits an optical spectrum which mimics quite much that of single graphene.

Keywords: graphene; pentacene; photovoltaics; ferroelectric π-stacking; optical properties

1. Introduction

Graphene is one of the frontier materials for flexible electronics, including photovoltaics. It has been used inside composite solar cells, either as the electrode when doped with N or B [1] or as the optically active part [2], as well as the hole transporting layer and even barrier for H_2O in order to

improve the resistivity against moisture [3]. As a substrate for the organic layers, graphene brings molecules into order [4], and therefore sets rules for the molecular pattern [5].

When molecules with the dipole groups are adsorbed at graphene, they induce the electric field which shifts the electronic density of the graphene layer according to the Stark effect. In the result, the dipole moment of about 2.1 Debye is induced in the graphene layer and its work function changes by about 1.5 eV [6] due to Wigner and Bardeen mechanism [7]. The dipole groups of molecules tend to align in the ferroelectric order in 1D π-stacks or 2D layers. Moreover, such ferroelectric organic layers possess other properties which are desired for applications in the solar devices. One of them is a cascade alignment of the energy levels of subsequent molecular layers, both in the valence-band and conduction-band manifold [6]. These cascade states simultaneously play a role of the donors or acceptors, depending on a direction from which the carriers arrive. Importantly, the π-stacks of these molecules transport electrons and holes through different parts in space, the mesogenic aromatic rings and the terminal dipole groups, respectively [8]. Thus, such separation of the carrier paths allows to decrease the charge recombination, which is the main problem restricting the power conversion efficiency.

In this theoretical work, we study the effect of a graphene substrate on the absorption spectra of pentacene decorated with the $–CH_2CN$ and –COOH dipole groups. The optical properties of undoped pentacene were studied with *ab initio* methods by other authors in relation to the charge transfer between the molecule and a TiO_2 substrate [9]. It has been reported that this molecule has a HOMO–LUMO gap within the range of solar radiation and that the dipole groups do not change much this gap [10]. On the other hand, experimental and theoretical studies about 2D organic networks at highly oriented pyrolytic graphite (HOPG) surface, which is very similar to graphene, reported the possibility to achieve tunable band gaps by a modification of the number of the aromatic rings [11]. For these reasons, the chosen molecule is a very good candidate to build organic layers for efficient photovoltaic cells with a graphene transparent electrode.

2. Materials and Methods

We considered the pentacene molecule decorated with four COOH and six CH_2CN dipole groups, with the rest of bonds saturated with hydrogen; in what follows, we will refer to this molecule as d-pentacene. It will be shown below that the optical spectrum of the molecule depends on both its own geometry and its electrostatic interactions with the graphene layer. To study these effects, we considered three arrangements: 1) plane molecule, with an “ideal” geometry optimized in vacuum (Pi), 2) the molecule calculated in vacuum but with the ”relaxed” geometry, assumed to be the same as that of the molecule placed on top of the graphene layer (Pr), and 3) the molecule with the geometry optimized on top of the graphene layer (PrG).

Density functional theory (DFT) calculations have been performed using the plane-wave pseudopotential code Quantum ESPRESSO [12]. The Perdew-Burke-Ernzerhof parametrization for the exchange-correlation functional has been used [13]. Norm-conserving pseudopotentials with a plane-wave energy cutoff of 60 Ry have been used for all atomic species. The uniform $2 \times 2 \times 1$ Monkhorst-Pack k-mesh [14] sufficed to sample the first Brillouin zone for the almost-square supercells, of planar side of around 20 Å; a comparison between this mesh and $6 \times 6 \times 1$ k-mesh for the projected DOS is reported in Figure S1 in the supporting information. A vacuum of 30 Å

separated the periodic slabs. The geometry optimization was achieved by allowing the graphene + molecule system to relax following the Broyden-Fletcher-Goldfarb-Shanno algorithm [15] until the forces on each atom decreased below 1×10^{-3} eV/Å.

The dielectric matrix has been calculated, in the linear response regime and within the random phase approximation (RPA), using the Yambo code [16]. In all cases, local field effects up to 14 eV were considered for the response function. Calculations of the dielectric matrix involved 1000 valence + conduction bands. A damping energy parameter of 0.1 eV was used to mimic experimental peak widths. Polarization of light was assumed to be polarized along the [110] direction, parallel to the graphene layer.

3. Results and Discussion

3.1. Geometric Characteristics

Figure 1a shows views of the isolated d-pentacene molecule (top) and that adsorbed at graphene (bottom); Figure 1b shows a top view of the adsorbed molecule. We thought primarily about the nature of the molecule adsorption, that is, whether it was chemisorption or any kind of physisorption. In principle, one would expect chemisorption to take place, provided that the molecule is close enough to the graphene layer. Thus, we placed initially a plane d-pentacene molecule close to graphene, with the C(ring)–C(graphene) and O(molecule)–C(graphene) distances being 2.0 Å and 1.48 Å, respectively. Besides, we located the hydrogen atoms of the –COOH groups far away from the graphene layer, to ease the O(pentacene)–C(graphene) bonding in case that it happened. After relaxation, we found the molecule to be repeled and distorted by graphene, with the distances between the central and outermost C atoms of d-pentacene and the graphene layer being 2.98 Å and 3.76 Å, respectively.

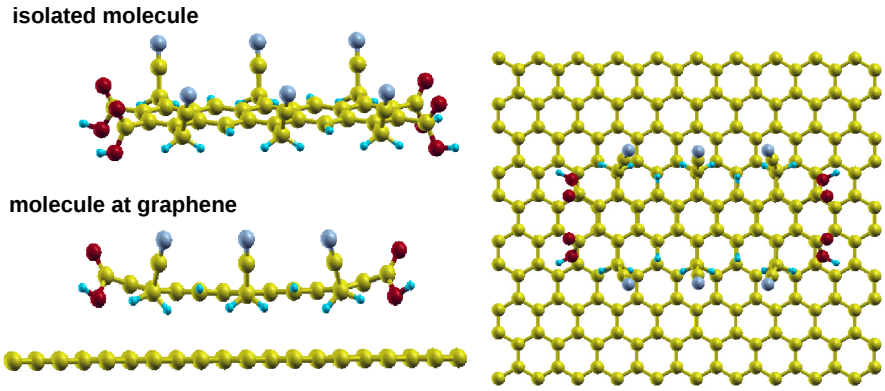

Figure 1. a) The atomic structure of an isolated d-pentacene molecule (top) and the molecule adsorbed on graphene (bottom). b) Top view of the latter. Carbon atoms appear in yellow, nitrogen and oxygen ones appear in grey and red, respectively, and hydrogen in cyan.

In addition, the hydrogen atoms from the –COOH groups swapped their positions, and got bound to the oxygen atoms closer to graphene. This way, the dipole moment of the –COOH aligned with that

of the CH_2CN group, in agreement with a previous work where the ferroelectric structure of a similar molecule, with just one C-ring and the same dipoles, was lower in energy than any other configuration of dipoles [6]. The optimization process is schematized in Figure 2, which displays details of the initial –COOH configuration as well as five transient stages of the atomic structure. It is interesting to inquiry about why hydrogen atoms swap their positions. In our opinion, this could be caused by the need of the system to align the different dipoles of the molecule. Indeed, the $–CH_2CN$ groups have dipole moments, which induce an electric field in the molecule; the hydrogen atoms then swap to screen such a field. Incidentally, the fact that graphene is slightly negative would help it to attract hydrogens as well. We checked that the geometry optimized with the method containing the self-interaction correction, namely the pSIC approach [17, 18], also swaps the hydrogens to place them at lower oxygens of the COOH group.

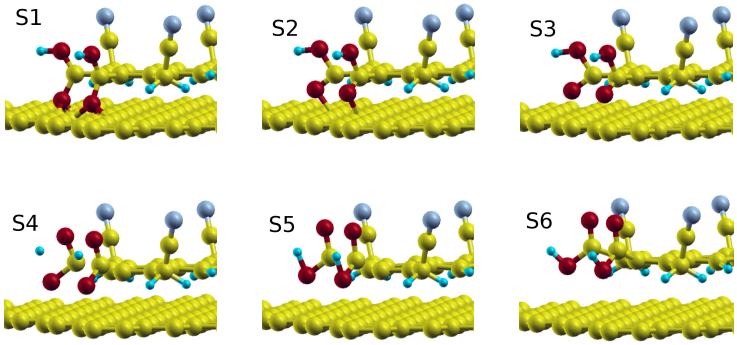

Figure 2. The initial (S1) and five transient atomic structures (S2–S6) during the optimization of the geometry of the molecule adsorbed at graphene. The color code is the same as for Figure 1.

In conclusion, our results indicate that d-pentacene is physisorped on graphene, and that adsorption is accompanied by a distortion of the molecule, which adopt a "cone"-like configuration with the –COOH groups further from graphene than the rest of the molecule.

3.2. Electronic Structure of Decorated Pentacene

Adsorption of d-pentacene onto graphene is accompanied by charge transfer from the molecule to the substrate. Figures 3a and 3b display the differential electronic density maps within the plane of graphene and the d-pentacene central part, respectively. The charge density is the electronic density multiplied by -e. These maps show difference between the actual electronic density of the system and that of the isolated substrate or molecule. The substrate is negatively charged, which agrees with previous studies for a similar but smaller molecule (with the same dipole groups) placed between two graphene sheets [6]; in that case, the bottom layer was shown to play a role of the cathode. Besides, the charge distribution within the substrate is quite delocalized. The change of the charge distribution induced in d-pentacene is positive in the central part and negative around the dipole groups and adjacent carbons. This map supports the scenario of separated paths for electrons and holes transport when the molecule is between the graphene electrodes, as has been previously discussed for the smaller molecule [8].

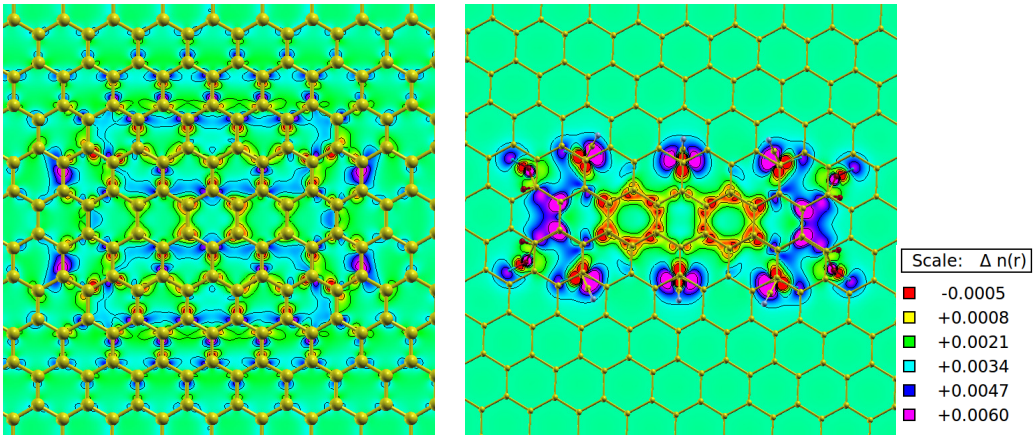

(a) (b)

Figure 3. The electronic density differential maps for graphene modified by the molecule (a) and molecule modified by graphene (b). The scale (right panel) is the same in both cases.

The above results suggest that the physical behavior of d-pentacene adsorbed at graphene is affected by two effects: the geometry of the molecule, which changes upon adsorption, and the electrostatic interactions between the molecule and the substrate. Both effects are obviously related, since the geometrical changes are caused in turn by the electrostatic interactions. However, it is convenient to consider them separately to identify how they affect the electronic structure and the optical properties of the entire system. Therefore, we considered the three models described in the Materials and Methods section: Pi (isolated d-pentacene with its "ideal" plane geometry), PrG (d-pentacene adsorbed on graphene, with its "relaxed" geometry), and Pr (isolated d-pentacene with the same geometry as for PrG). Thus, comparison between Pi and Pr provides information about an effect of the geometry, and that between Pr and PrG accounts for the effect of weak π-bonds with the graphene substrate.

Figure 4 shows the densities of states (DOS) for these three configurations; the origin of energies was taken as the corresponding Fermi energy for each case. Figure 4a plots the DOS for the Pi and Pr configurations. This figure gives an evidence that the geometry optimization of the molecule changes the distribution of the deep energy levels, but not those close to the HOMO–LUMO gap; in particular, the HOMO remains unchanged (note that the red line overlaps with the blue one in Figure 4a). As for the LUMO, it is shifted upwards by about 0.2 eV, likely due to dipolar interactions within the molecule. In particular, the HOMO–LUMO gaps are $\varepsilon_{HO-LU} = 0.81$ eV and $\varepsilon_{HO-LU} = 1.02$ eV for Pi and Pr, respectively. Figure 4a also shows that the geometry optimization does not yield any charge transfer, since the Fermi energy remains unchanged relative to the HOMO. Figure 4b, on its part, compares the DOS for Pr and PrG cases. The electrostatic interactions with the substrate now shift upwards the Fermi energy, as one would expect given the donor character of the molecule that we have already mentioned. The remaining DOS is almost rigidly shifted downwards, what causes the system to become metallic. These plots demonstrate then that the changes in the molecular levels are mainly associated to the geometrical distortions. In essence, the effect of the substrate is the (roughly) rigid shift downwards of the entire DOS accompanying the charge transfer.

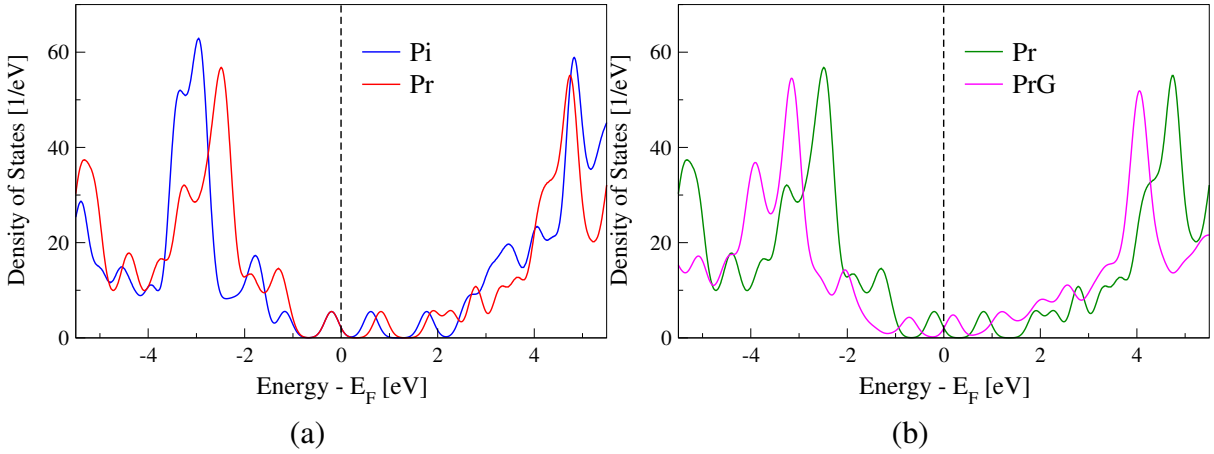

Figure 4. Comparative densities of states: Pi and Pr configurations (a) and Pr and PrG ones (b).

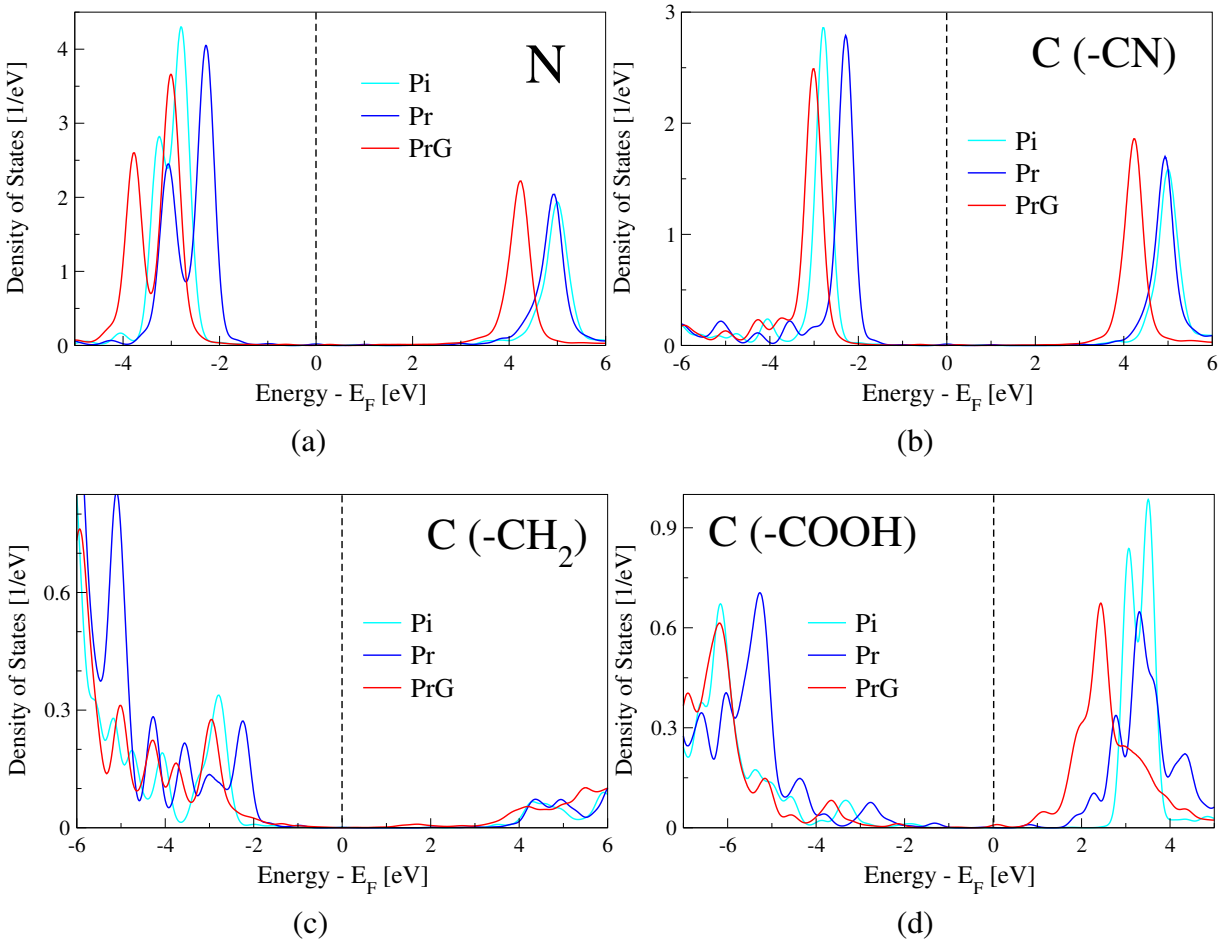

Figure 5. Projected DOS at N (a) and C of –CN (b), –CH_2 (c), –COOH groups (d) for Pi, Pr and PrG.

Deeper insights into the electronic structure of the system are provided by the projection of the DOS onto selected atomic states. Figure 5 shows the projected DOS (pDOS) onto nitrogen (from the $–CH_2CN$ group) and three distinct carbon (from the cyano, methylene and carboxyl groups) atoms for the Pi, Pr and PrG cases. Geometry relaxation does not affect much the projection of the unoccupied levels onto CH_2CN states (Figures 5a to 5c), whereas it causes occupied states to shift upwards by about 0.5 eV. On the contrary, the change in geometry affects greatly the projection onto the carbon atom from the carboxyl group. We observe in Figure 5d that the projections onto unoccupied levels become wider after the molecule gets distorted whilst the projection with lower energy shifts downwards. As for the projections onto occupied levels, they shift upwards almost rigidly by effect of the geometry optimization. On the other hand, the electrostatic interactions with the graphene layer cause essentially a rigid shift downwards of the projections in all cases.

Figures 6a and 6b show the projection of the DOS onto non-equivalent oxygen atoms of the –COOH groups for the Pi, Pr and PrG configurations. One of these oxygens (labeled as O_{up}) is doubly bonded to the carbon atom, whereas the other (O_{dw}) is singly bounded to carbon and to a hydrogen atom as well. This is the reason why they show different chemical behavior. As for the previous figures, the main effect seems to come from the geometrical distortion of the molecule. Indeed, Figure 6a reveals a widening and shift downwards of the unoccupied levels, which is more pronounced for O_{up}, in Pr compared to Pi. On the contrary, and also as before, physisorption causes just a roughly shift downwards of the levels, with no apparent changes in their structure, as shown in Figure 6b. This is an indirect evidence that $\pi-$bonds are indeed established between the molecule and the graphene substrate.

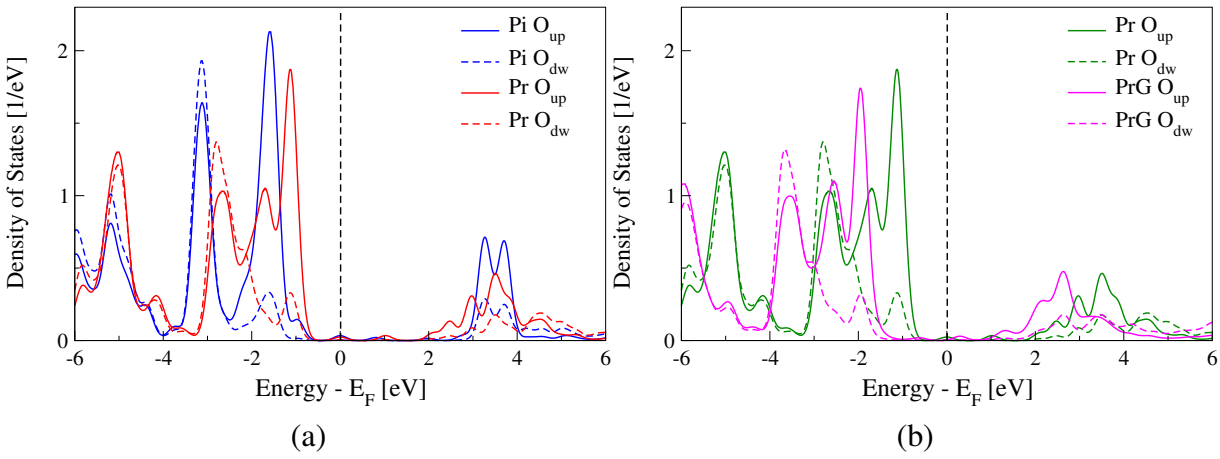

Figure 6. PDOS onto oxygen states. Comparative between Pi and Pr (a) and Pr and PrG (b) configurations.

3.3. Modified Chemical Structure

From the previous results, the question arises as to how to modify the electronic structure of the d-pentacene + graphene system to increase the optical efficiency through some "levels engineering". A quick response would be to change the dipole groups; one could then try different possibilities and check which one yields a suitable HOMO–LUMO gap. We have explored here a different approach: we have investigated an effect of changing the C–H single bonds within the d-pentacene molecule by

either C–OH or C=O bonds. In the first case, even though one still have a single bond, the oxygen atom is likely to enrich the electrostatic interactions (within the molecule and between the molecule and the graphene sheet) because of its higher number of electrons. In the second case one has a double bond which "fixes" the single-double bonds pattern of each aromatic ring, thus avoiding the Kekule-structures duality. In this case, the electrons can no longer be considered as delocalized within these rings, what incidentally decreases the aromaticity. Figure 7 shows schematics of the original d-pentacene as well as its two modifications; in what follows, we will label them as molecules A, B and C, respectively.

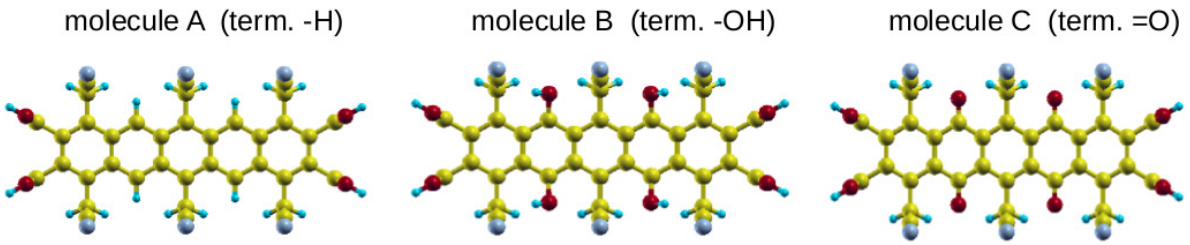

Figure 7. Atomic structure of the original d-pentacene (left) and its modifications: replacement of H with –OH (middle) and =O (right). The color code is the same as for Figure 1.

The proximity of the graphene layer to the modified molecules depend on their particular chemical conformation. For molecule B, the proximity of graphene causes additional perpendicular $\pi-$bonds to appear, and therefore a weakening of the double $\pi-$bonds in the planar mesogenic part of the molecule. For molecule C, we find weaker $\pi-$bonds in the mesogenic part, caused now by the double (instead of single) planar saturation bonds.

Figures 8a and 8b display the DOS of d-pentacene, in its "ideal" undistorted structure, at various distances from graphene and a comparison of the electronic structures of molecules A, B, C located at 4.5 Å from graphene, respectively. Interestingly, a peak at the Fermi level appears when the original d-pentacene is very close to graphene (Figure 8a) and when the molecule is modified with =O double bonds (Figure 8b). Both effects, i.e., the formation of the perpendicular π-bonds and additional planar π-bonds, cause the aforementioned weakening of the bonds in the mesogenic part. Consequently, as we expected, the chemical modifications of the terminal parts can be used for engineering of the optical spectra.

Figure 9 shows the DOS projected onto selected parts of the A, B and C molecules, as well as the molecule A in various distances from graphene. According to our intuitive guess, the non-zero DOS values at ε_F arise from the C atoms of the central rings. A small contribution to the DOS at ε_F from the –COOH group, as well as contribution of the additional oxygens for molecule C, appears when the molecule and graphene are about 2.5 Å away. For the most distant molecular part, namely the cyano group, the charge redistribution due to the perpendicular π-bonds with graphene does not affect the pDOS. This is in contrast to the terminal chemical modifications, which shift the peaks and change their width for both the occupied and unoccupied N-states.

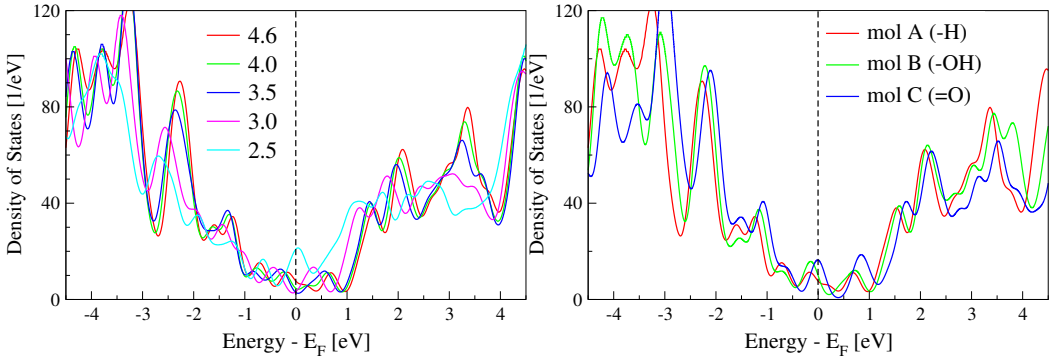

Figure 8. DOS of d-pentacene at graphene in various distances (a), and DOS of three modifications of d-pentacene (see Figure 7) (b).

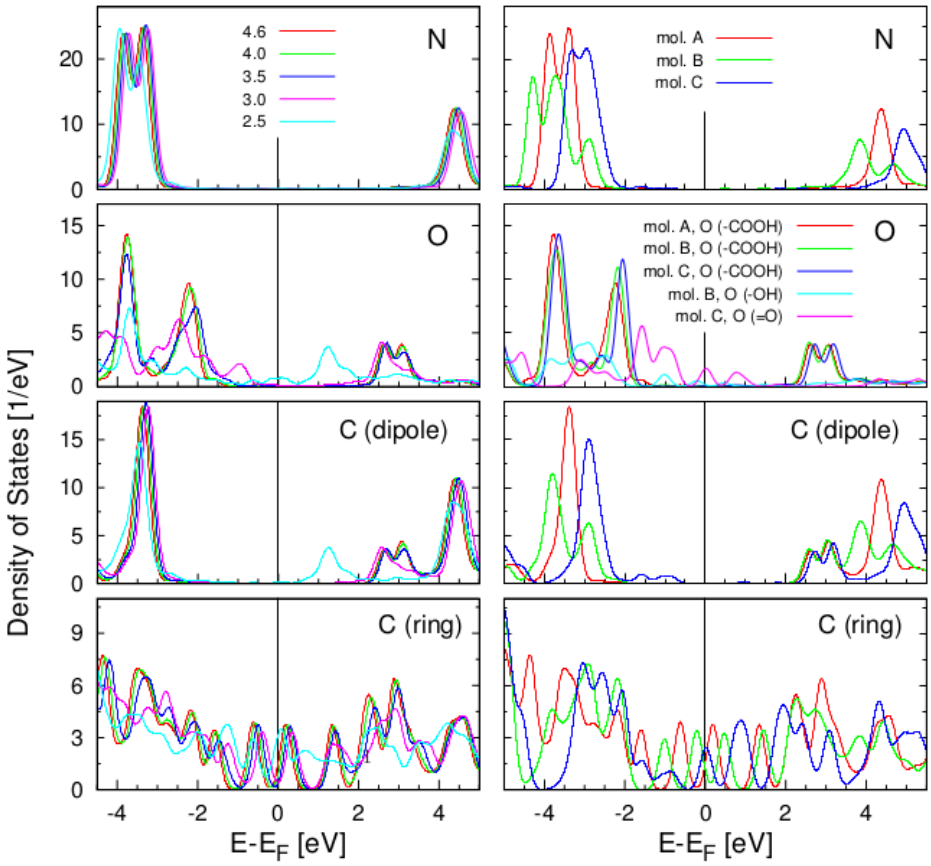

Figure 9. The density of states projected at N, O, and C of the dipoles and the central rings for the molecule A in various distances from graphene (left panels) and the same projections for the molecules A, B, C at graphene in the distance 4.6 Å (right panels). The contributions of the O-states from the terminal moieties –OH and =O of the molecules B and C, respectively, are also displayed.

3.4. Optical Properties

The optical properties of isolated d-pentacene in its "ideal" and "relaxed" geometries (that is, Pi and Pr, respectively), as well as those of the molecule adsorbed at graphene (PrG), were studied within the linear response theory under the RPA. Figure 10 (upper panel) shows the imaginary part of the RPA or "interacting" dielectric function $\varepsilon(\omega)$. This imaginary part is proportional to the optical absorption coefficient. For comparison purposes, we computed the non-interacting, that is, corresponding to a system of independent particles dielectric function $\varepsilon_0(\omega)$ as well; this is shown in Figure 10 (bottom panel).

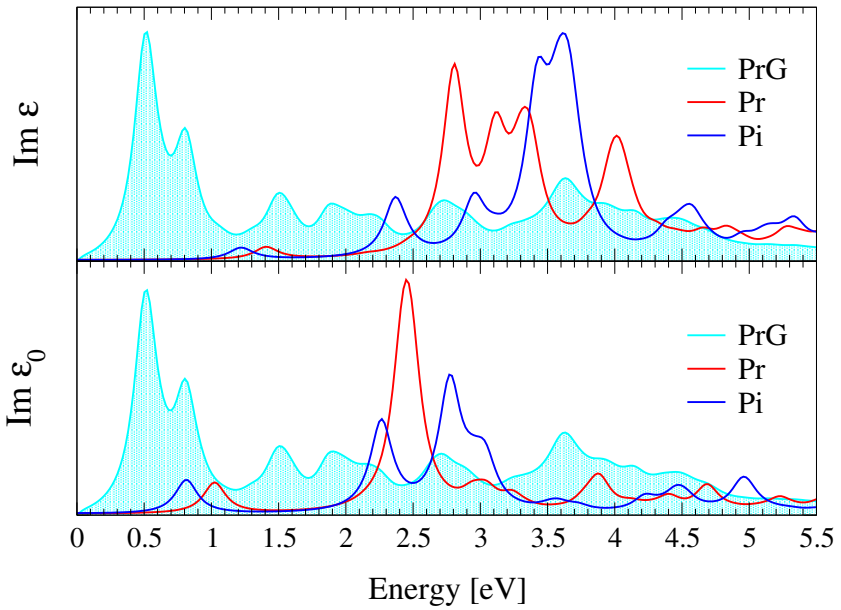

Figure 10. The interacting (ε) and noninteracting (ε_0) dielectric functions for Pi, Pr and PrG.

The first (lowest energy) peaks of the noninteracting dielectric function of isolated molecules correlate with the corresponding HOMO–LUMO gaps, 0.8 eV for Pi and 1.0 eV for Pr. The pDOS in this energetic region suggests that the optical transitions occur between the pentacene-chain localized states. These peaks have very low intensities, what is probably related to the dipole-symmetry-based transition rules. The group of intense peaks in the noninteracting dielectric function, roughly between 2.0 and 4.0 eV, could correspond to excitations from valence band states localized at dipole-groups to conduction band states correlated to d-pentacene rings, as well as from valence band states centered at the d-pentacene core to conduction band states centered at dipoles. In the PDOS, most of Pi high-density states are further from the Fermi energy than the corresponding states for Pr, although some low-density states are closer to ε_F. These features correlate with the noninteracting dielectric functions of the appropriate cases.

Compared to its noninteracting counterpart, and in very general sense, the peaks of the interacting dielectric function are generally wider than those of ε_0. For the Pi configuration, the peak exhibited by ε_0 at 2.3 eV remains unchanged in ϵ; however, peaks at higher energy shift to the blue light. More interesting is the situation for Pr. In this case, it is the peak at around 4.0 eV which remains roughly

unchanged, whereas the intense peak of ε_0 at 2.5 eV is splitted into three peaks within the 2.8–3.4 eV range. We remark two additional characteristics. The first is that the peaks for the HOMO–LUMO transitions, which are little intense, but apparent in the noninteracting case, do not appear in the interacting spectrum, which indicates that the direct transitions mediated by the screened potential are forbidden (we recall that we are accepting the RPA). The second characteristic is that, contrarily to the non-interacting case, molecular distortions cause a shift to the blue light, by about 0.5 eV, in the interacting case.

The spectrum of d-pentacene at graphene (PrG) does not vary much between the noninteracting and interacting cases, as shown in Figure 10, and it does not show prominent features which could be assigned to the electrostatic interactions between the molecule and the substrate either. Moreover, the graphene-based transitions are so rich that it is difficult to find the molecular and the molecule-to-graphene transitions. This is demonstrated in Figure 11, where the imaginary part of the interacting dielectric function of the PrG configuration is compared to that of the graphene layer (without any adsorbed molecule). This plot shows that the spectrum of PrG practically mimics that of pure graphene. This is an effect of the large number of atoms in graphene substrate, and therefore the electronic states, which are optically active. However, Figure 11 shows a slight supression of the lowest transitions within the substrate. Thus, the optical transitions between d-pentacene and graphene seem to cause a slight shift to the right for the low-energy part of the PrG spectrum, as well as the intensification of this spectrum in the region below the HOMO–LUMO gap of the molecule.

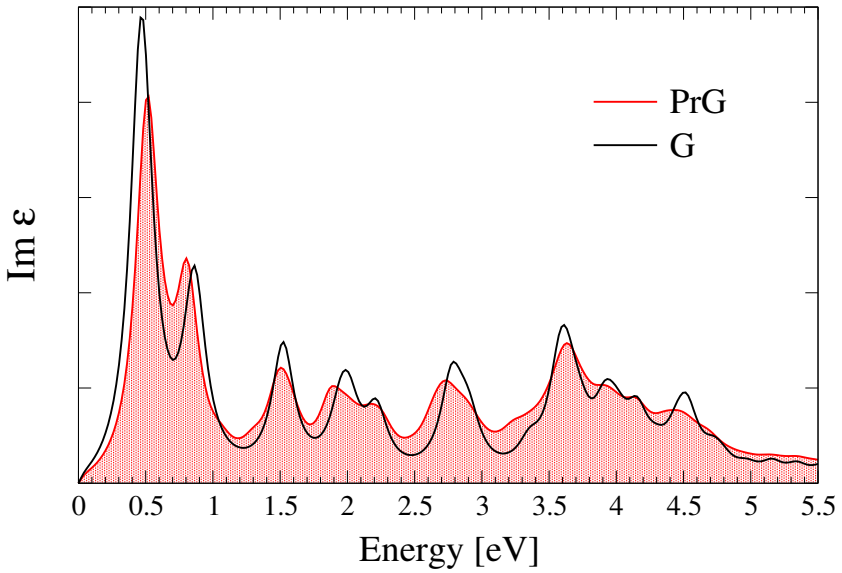

Figure 11. Comparison between the interacting dielectric function of PrG and that of graphene calculated in the same cell as PrG.

In any case, the analysis of the optical response is consistent with our previous discussion in the sense that the most remarkable physical change in the system arises from the molecular distortions, and not from interactions with the graphene substrate. Of course, the analysis of optical properties in the system is far to be conclusive, since the energy levels have been calculated within "standard" DFT, ignoring many-body corrections. In particular, the possibility of excitonic resonances is not taken into account in RPA. However, this study could open a research field not only about the role of

intermolecular interactions in this type of system, but also about possible "levels engineering" strategies.

4. Conclusions

The spectroscopic properties of a photovoltaic molecule, namely pentacene decorated with four COOH and six CH_2CN dipole groups and adsorbed at a graphene substrate have been studied by *ab initio* methods: DFT and RPA for the dielectric function.

Our results show that chemisorption does not occur; instead, physisorption accompanied by a "cone"-like distortion of the molecule takes place. A charge transfer from d-pentacene to graphene is correlated with charge redistribution within the molecule, where the central part yields electrons to the dipole terminal groups. In general terms, the effect of the molecular distortion shifts the electronic spectrum upwards, while the weak π-bonding with the substrate manifests itself in the opposite way.

The chemical modification of the saturation from –H terminal to the electron-rich –OH and =O terminals changes the single-double bond pattern in the central part of d-pentacene, leading to smaller HOMO–LUMO gaps. The same effect is observed for the π-bonds between the molecule and graphene at small distances. This observation can be used in the "engineering" of the optical spectra. It is remarkable that these molecules have their lowest appreciable transitions at relatively high energy, what makes them not optimal for efficient photovoltaics.

Trends in the features of the dielectric function correspond to those drawn from the projected density of states. In particular, one sees that important changes appear in the optical absorption spectrum after the molecule gets distorted. However, adsorption of the molecule does not result in significant changes in the optical absorption spectrum with respect to that for single graphene. Further discussion of the optical behaviour would require more sophisticated theoretical schemes which would include particle-hole interactions.

Acknowledgments

Calculations have been performed in the Cyfronet Computer Centre using the Prometheus computer, which is a part of the PL-Grid Infrastructure. This work has been supported by The National Science Centre of Poland (the Projects: 2013/11/B/ST3/04041 and DEC-2012/07/B/ST3/03412) and by the Junta of Extremadura through Grant GR15105.

Conflict of Interest

The authors declare that there is no conflict of interest regarding the publication of this paper.

References

1. Rashid bin Mohd Yusoff A, Dai L, Cheng HM, et al. (2015) Graphene based energy devices. *Nanoscale* 7: 6881–6882.
2. Ozyilmaz B, Saha S, Toh CT, et al. (2013) Photovoltaic cell with graphene-ferroelectric electrode. United States Patent Application US 14/385, 680.

3. Loh KP, Tong SW, Wu J (2016) Graphene and graphene-like molecules: prospects in solar cells. *J Am Chem Soc* 138: 1095–1102.
4. Reinert F (2013) Graphene gets molecules into order. *Nat Phys* 9: 321–322.
5. Colson J W, Woll AR, Mukherjee A, et al. (2011) Oriented 2D covalent organic framework thin films on single-layer graphene. *Science* 332: 228–231.
6. Wierzbowska M, Wawrzyniak-Adamczewska M (2016) Cascade Donor-Acceptor Organic Ferroelectric Layers, between Graphene Sheets, for Solar Cell Applications. *RSC Adv* 6: 49988–49994.
7. Wigner E, Bardeen J (1935) Theory of the Work Functions of Monovalent Metals. *Phys Rev* 48: 84.
8. Wawrzyniak-Adamczewska M, Wierzbowska M (2016) Separate-Path electron and hole transport across π-stacked ferroelectrics for photovoltaic applications. *J Phys Chem C* 120: 7748–7756.
9. Ljungberg MP, Vänskä O, Koval P, et al. (2016) Charge transfer states at the interface of the pentacene monolayer on TiO_2 and their influence on the optical spectrum. Available from: http://www.arXiv.org/abs/1610.01789.
10. Masiak PM, Wierzbowska M (2017) Ferroelectric π-stacks of molecules with the energy gaps in the sunlight range. *J Mater Sci* [In Press].
11. Xu L, Yu Y, Lin J, et al. (2016) On-surface synthesis of two-dimensional imine polymers with a tunable band gap: a combined STM, DFT and Monte Carlo investigation. *Nanoscale* 8: 8568.
12. Giannozzi P, Baroni S, Bonini N, et al. (2009) QUANTUM ESPRESSO: a modular and open-source software project for quantum simulation of materials. *J Phys: Condens Matter* 21: 395502.
13. Perdew JP, Burke K, Ernzerhof M (1996) Generalized Gradient Approximation made simple. *Phys Rev Lett* 77: 3865–3868.
14. Monkhorst HD, Pack JD (1976) Special points for Brillouin-zone integrations. *Phys Rev B* 13: 5188–5192.
15. Fletcher R (1987) *Practical methods of optimization*, 2nd. Eds., John Wiley & sons, Chichester, UK.
16. Marini A, Hogan C, Grüning M, et al. (2009) YAMBO: an *ab initio* tool for excited state calculations. *Comp Phys Comm* 180: 1392–1403.
17. Filippetti A, Spaldin NA (2003) Self-interaction-corrected pseudopotential scheme for magnetic and strongly-correlated systems. *Phys Rev B* 67: 125109.
18. Wierzbowska M, Majewski JA (2011) Forces and Atomic Relaxation in Density Functional Theory with the Pseudopotential Self-Interaction Correction. *Phys Rev B* 84: 245129.

AIMS Press